# Universiteit Leiden
## The Netherlands

# Malaria parasite evades mosquito immunity by glutaminyl cyclase-mediated posttranslational protein modification

Kolli, S.K.; Molina-Cruz, A.; Araki, T.; Geurten, F.J.A.; Ramesar, J.; Chevalley-Maurel, S.; ... ; Janse, C.J.

# Malaria parasite evades mosquito immunity by glutaminyl cyclase–mediated posttranslational protein modification

Surendra Kumar Kolli[a,1,2] , Alvaro Molina-Cruz[b] , Tamasa Araki[c], Fiona J. A. Geurten[a], Jai Ramesar[a], Severine Chevalley-Maurel[a], Hans J. Kroeze[a], Sascha Bezemer[a], Clarize de Korne[a,d], Roxanne Withers[b], Nadia Raytselis[b], Angela F. El Hebieshy[e,f], Robbert Q. Kim[e,f], Matthew A. Child[g] , Soichiro Kakuta[h], Hajime Hisaeda[c], Hirotaka Kobayashi[i], Takeshi Annoura[c], Paul J. Hensbergen[j] , Blandine M. Franke-Fayard[a], Carolina Barillas-Mury[b,1] , Ferenc A. Scheeren[k,1], and Chris J. Janse[a,1]

Glutaminyl cyclase (QC) modifies N-terminal glutamine or glutamic acid residues of target proteins into cyclic pyroglutamic acid (pGlu). Here, we report the biochemical and functional analysis of *Plasmodium* QC. We show that sporozoites of QC-null mutants of rodent and human malaria parasites are recognized by the mosquito immune system and melanized when they reach the hemocoel. Detailed analyses of rodent malaria QC-null mutants showed that sporozoite numbers in salivary glands are reduced in mosquitoes infected with QC-null or QC catalytically dead mutants. This phenotype can be rescued by genetic complementation or by disrupting mosquito melanization or phagocytosis by hemocytes. Mutation of a single QC-target glutamine of the major sporozoite surface protein (circumsporozoite protein; CSP) of the rodent parasite *Plasmodium berghei* also results in melanization of sporozoites. These findings indicate that QC-mediated posttranslational modification of surface proteins underlies evasion of killing of sporozoites by the mosquito immune system.

glutaminyl cyclase | pyroglutamic acid | immune evasion | sporozoite | melanization

N-terminal modification of glutamine or glutamic acid residues to pyroglutamic acid (pGlu; 5-oxo-L-proline) is a posttranslational modification of proteins, catalyzed by glutaminyl cyclases (QCs) found in eukaryotes and prokaryotes (1, 2). Two evolutionarily unrelated classes exist, represented by mammalian QC enzymes and QC enzymes present in bacteria, plants, and parasites (3). These two classes of QC enzymes share no sequence homology, supporting a different evolutionary origin. Mammalian cells can express two forms, the secreted glutaminyl-peptide cyclotransferase (QPCT) or its iso-enzyme QPCTL, localized in the Golgi complex. pGlu is implicated in maturation and stabilization of mammalian proteins such as neuropeptides and cytokines (3, 4). QC activity has been associated in humans with pathological processes such as amyloidotic diseases (3–6). Recently, it has been shown that QPCTL is critical for pGlu formation on the N terminus of CD47 which facilitates myeloid immune evasion as it is essential for binding of myeloid inhibitory immune receptor SIRPα (7, 8). The physiological function of QCs in plants, bacteria, and parasites remains poorly characterized. Several pGlu-containing proteins of plants are involved in defense reactions against pathogens (3). The function of QCs in parasites is unknown.

Here, we report the biochemical and functional analysis of QC of malaria parasites. Malaria parasites are unicellular apicomplexan parasites with a complex life cycle involving an *Anopheles* mosquito and a vertebrate host. We show that QC plays a role in life cycle stages that are responsible for transmission between vertebrate hosts by the mosquito. Transmission occurs when gametocytes, formed in the blood of the vertebrate host, develop into gametes when taken up by a mosquito and fuse to form zygotes. Zygotes transform into ookinetes that cross the midgut epithelial cells and develop into oocysts in the hemocoel (9). Sporozoites, formed inside oocysts, are released into the hemocoel and invade salivary glands for transmission to a new vertebrate host (10, 11). Mosquito innate immune responses in the hemocoel can detect and eliminate malaria parasites through multiple effector mechanisms (12, 13). Immune responses that target the ookinete stage have been studied in detail and involve activation of nitration responses by invaded midgut cells (13) and local release of hemocyte-derived microvesicles that promote complement activation (14). In addition, thioester-containing protein 1 (TEP1), a key effector of mosquito complement, binds to the ookinete surface, thereby initiating the formation of a complex that kills the parasite through lysis or melanization (15). Whereas melanotic encapsulation of ookinetes is an important mosquito anti-*Plasmodium* immune effector response (12, 16, 17), extensive melanization of other life cycle stages in the mosquito, such as oocysts or sporozoites, has not been reported. We show

## Significance

Chemical modification of some proteins by the enzyme glutaminyl cyclase (QC) modulates important processes in humans, including immune evasion by malignant cells. We found that a QC enzyme is also active in malaria parasite stages developing in the mosquito. Mutant parasites that lack QC activity are eliminated by encapsulation as they transit from the midgut to the salivary glands. Disrupting the mosquito encapsulation response allows parasites to survive, indicating that QC-mediated modifications prevent immune recognition. We provide direct evidence that a specific modification of a major surface protein of the malaria parasite by QC is important for survival. Understanding how malaria parasites evade mosquito immunity could open the possibility to designing novel strategies to disrupt malaria transmission.

[1]To whom correspondence may be addressed. Email: kollis24@usf.edu, cbarillas@niaid.nih.gov, f.a.scheeren@lumc.nl, or c.j.janse@lumc.nl.

[2]Present address: Center for Global Health and Infectious Diseases Research, College of Public Health, University of South Florida, Tampa, FL 33612.

here that *Plasmodium* QC plays a role in sporozoite immune evasion by preventing melanization and provide direct evidence that QC-mediated posttranslational modification of a sporozoite surface protein is critical to escape immune recognition and elimination.

## Results

**_Plasmodium_ QC Shows Sequence Homology to Bacterial and Plant QCs, Has Cyclase Activity, and Is Expressed in Transmission Stages.** A single gene encoding a QC, named QPCT, has been identified by electronic annotation in all sequenced *Plasmodium* genomes. *Plasmodium* QCs have a size ranging from 352 to 384 amino acids and share 70 to 76% sequence similarity and 50 to 54% identity (*SI Appendix,* Fig. S1*A*). *Plasmodium* QC has no protein export domains but contains a transmembrane domain (N-terminal, 42 to 57 amino acids) (*SI Appendix,* Fig. S1*C*). QC of the human malaria parasite *Plasmodium falciparum* (*Pf*QC) shows 21 to 27% identity to QCs of various bacteria and the plant *Carica papaya* (*Cp*QC) (1, 18–20) (*SI Appendix,* Fig. S1*B*). All nine amino acids of the catalytic site of bacterial and plant QCs (1) are conserved in *Plasmodium* QC, and the secondary structure of *Pf*QC, threaded against *Cp*QC and bacterial QCs, reveals 22 conserved β-sheets (*SI Appendix,* Fig. S1*C*). A *Pf*QC three-dimensional (3D) homology model, built against *Cp*QC and bacteria QCs, predicted five conserved blades of antiparallel β-sheets and a highly similar tertiary structure of *Pf*QC and *Cp*QC (Fig. 1 *A* and *B* and *SI Appendix,* Fig. S1*D*). Recombinant wild-type (WT) *Pf*QC has cyclase activity in a two-step enzyme-activity assay that is not present in a catalytically dead *Pf*QC (*Pf*QC$^{CD}$), in which two conserved amino acid residues in the catalytic site were mutated (Fig. 1*C*).

Published expression data indicate that QC is expressed in gametocytes, ookinetes, oocysts, and sporozoites, *Plasmodium* mosquito stages critical for disease transmission (*SI Appendix,* Fig. S1 *E–G*). *Pf*QC is present in proteomes of female gametocytes, oocysts, and sporozoites, and *Plasmodium yoelii* QC (PY17X_1314500) has been detected in oocyst and sporozoite proteomes. *Pf*QC is also present in proteomes of sporozoite surface proteins (21). However, the protein has not been detected in asexual blood-stage proteomes. The presence of *Pf*QC in female gametocytes and sporozoites corresponds to increased transcript levels in female gametocytes and sporozoites (PlasmoDB v.46, http://www.plasmodb.org). Increased transcription of *Plasmodium berghei* QC (*Pb*QC; PBANKA_1310700) was also observed in gametocytes, zygotes/ookinetes, and sporozoites. Combined, the data on QC expression suggest a role of QC in stages responsible for mosquito transmission. QC expression in transmission stages was confirmed by analyzing a transgenic rodent malaria parasite (*P. berghei*; *Pbqc::cmyc*), expressing a cmyc-tagged QC (Fig. 1*D* and *SI Appendix,* Fig. S2 *A–E* and Table S1).

**Absence of QC Leads to Melanization of Rodent and Human Malaria Oocysts and Sporozoites.** To analyze QC function in vivo, QC-null mutants of the rodent parasite *P. berghei* and the human parasite *P. falciparum* were generated. QC-null mutants were created by deleting the *qc* gene from the parasite genome using standard methods of genetic modification. Blood stages of three *P. berghei* QC-null mutants (Δ*qc1*; Δ*qc2*; Δ*qc-G*) showed WT asexual growth rate and gametocyte production. In addition, gametocytes of QC-null mutants produced WT-like numbers of mature ookinetes in vitro (*SI Appendix,* Fig. S2 *F–J* and Table S1). All three *P. berghei* QC-null mutants constitutively express the reporters mCherry and luciferase. When fed to *Anopheles*
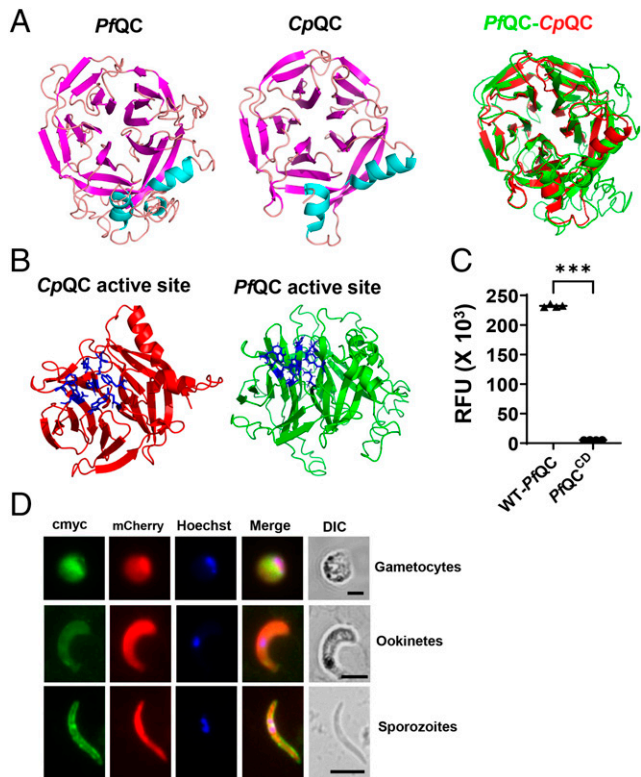


**Fig. 1.** Three-dimensional homology model, cyclase activity, and expression of *P. falciparum* QC. (*A*) Three-dimensional homology model of *P. falciparum* QC, generated against the resolved QC structures from *C. papaya* and *Z. mobilis*, and the 3D template structure of *C. papaya* QC. Structures are visualized using PyMOL. Helices, cyan; sheets, magenta; loops, brown. An overlay is shown of *Pf*QC (green) and *Cp*QC (red). (*B*) Visualization of the *Cp*QC catalytic site (blue), composed of active-site residues F22, Q24, F67, E69, W83, W110, N155, W169, and K225 and the predicted *Pf*QC (blue) catalytic site, based on the catalytic-site residues conserved with the *Cp*QC catalytic site (F107, Q109, F152, E154, Y174, Y200, N269, F285, and K349; *SI Appendix,* Fig. S1*D*). (*C*) Cyclase activity of *Pf*QC (relative fluorescence units, RFU), in an enzyme activity assay using recombinant wild-type (WT-*Pf*QC; $n = 4$) and cyclase-dead *Pf*QC (QC$^{CD}$; $n = 4$), containing two point mutations in the active site, F107A and Q109A (***$P < 0.0001$). (*D*) QC expression in gametocytes, ookinetes, and sporozoites, visualized by staining with anti-cmyc antibodies of fixed *Pbqc::cmyc* parasites that express cmyc-tagged QC and mCherry. Nuclei are stained with Hoechst 33342. DIC, differential interference contrast. (Scale bars, 5 μm.)

*stephensi*, QC-null parasites produced similar numbers of oocysts as WT parasites (Fig. 2*A* and *SI Appendix,* Table S1). Closer examination of maturing oocysts by light microscopy revealed the presence of aberrant, dark-colored mature oocysts in 55 to 65% of QC-null–infected mosquitoes (1 to 85 dark-colored oocysts per mosquito), while such oocysts were absent in WT-infected mosquitoes (Fig. 2 *A–D*). No dark-colored ookinetes/oocysts were detected before day 10 postinfection (p.i.). However, aberrant, enlarged, dark-colored sporozoites, either still inside or during release from oocysts, were observed between day 14 and 21 p.i. (Fig. 2*F* and *SI Appendix,* Fig. S2 *K–P*). Dark-colored oocysts and sporozoites indicate the formation of melanin, a dark, insoluble pigment. Melanotic encapsulation is an important mosquito anti-*Plasmodium* immune effector response (16, 17). To our knowledge, melanization of *P. berghei* sporozoites has not been observed before and only one report describes the melanization of *P. berghei* oocysts, resulting from replacement of the *P. berghei* gene encoding the circumsporozoite protein (*csp*) by the *csp* gene of the avian malaria parasite *Plasmodium gallinaceum* (22).

At day 21 p.i., nonmotile, enlarged sporozoites covered by melanin were found in the hemocoel, often in clusters or attached to salivary glands (Fig. 2 *G–I*). We found that the
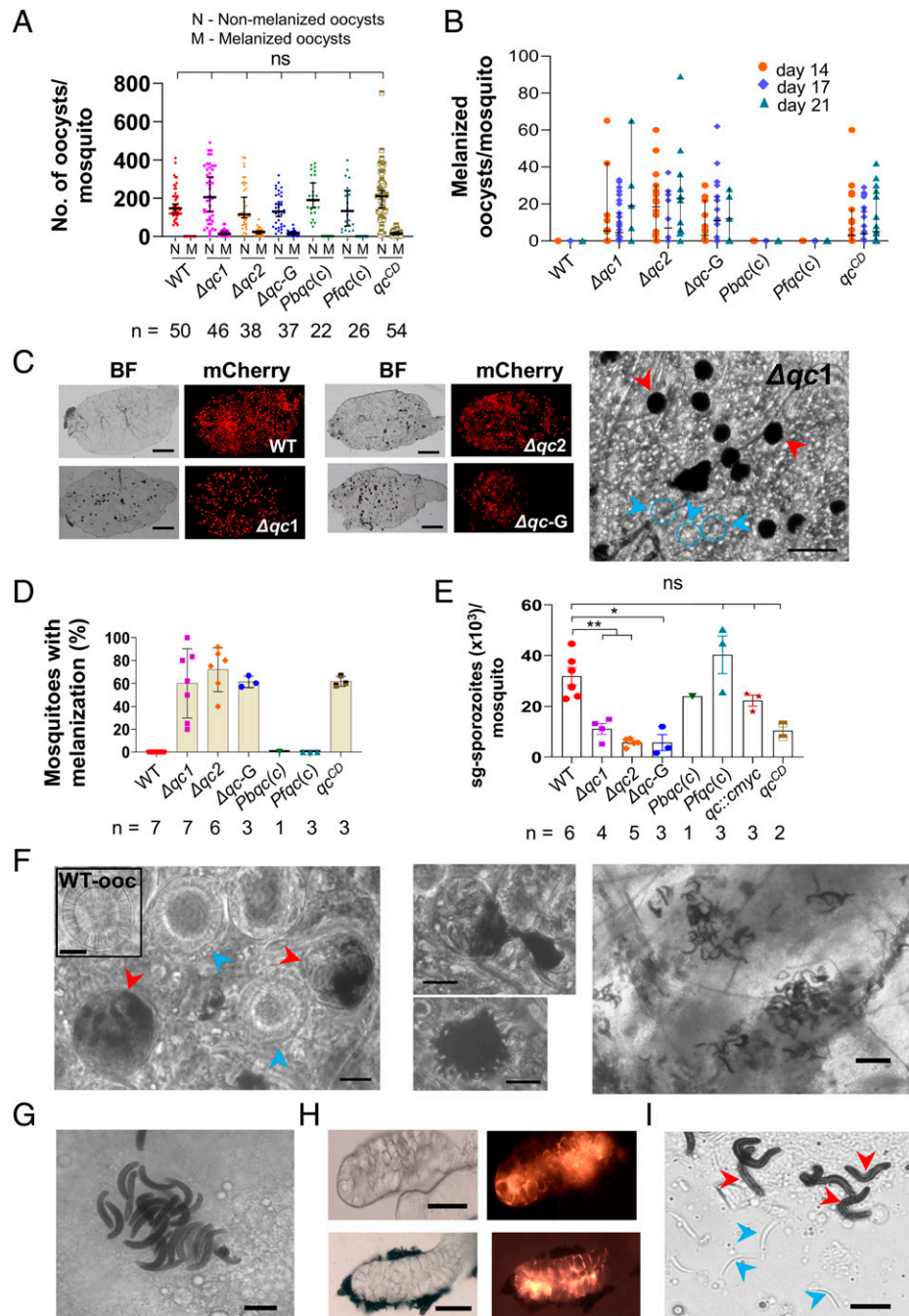
**Fig. 2.** Melanization of oocysts and sporozoites in mosquitoes infected with QC-null mutants and reduced sg-sporozoite numbers. (*A*) Number of melanized and nonmelanized oocysts per mosquito (median + 95% CI; *n*, number of mosquitoes) infected with QC-null mutants (Δ*qc*), QC-null mutants complemented with *P. berghei* or *P. falciparum* QC [*Pbqc*(c) and *Pfqc*(c)], or infected with a QC catalytically dead mutant (*qc^{CD}*). At least three replicates [except *Pbqc*(c): one experiment and *qc^{CD}* in duplicate] were pooled for statistical analysis. ns, not significant [Mann–Whitney *U* test; significance relative to WT; *P* values: Δ*qc*1 0.159, Δ*qc*2 0.174, Δ*qc*G 0.188, *Pbqc*(c) 0.360, *Pfqc*(c) 0.079, and *qc^{CD}* 0.062]. (*B*) Number of melanized oocysts per mosquito (day 14, 17, and 21) (*n* = 15 to 20) infected with *qc* mutants. Number of mosquitoes on day 14, 17, and 21: WT (18, 21, and 18); Δ*qc*1 (10, 32, and 5); Δ*qc*2 (16, 10, and 12); Δ*qc-G* (14, 18, and 5); *Pbqc*(c) (28, 11, and 18); *Pfqc*(c) (16, 19, and 22); *qc^{CD}* (17, 24, and 15). At least three replicates [except *Pbqc*(c): one experiment and *qc^{CD}* in duplicate] were pooled for statistical analysis and error bars represent the median with 95% CI. (*C*) Melanized oocyst in mosquito midguts (day 14) infected with QC-null mutants (Δ*qc*). Bright-field (BF) and fluorescence images of mCherry-expressing oocysts. (Scale bars, 200 μm.) (*C, Right*) Melanized (red arrowheads) and nonmelanized (blue arrowheads) oocysts in a Δ*qc1*-infected mosquito (day 14). Nonmelanized oocysts are shown in blue circles. (Scale bar, 100 μm.) (*D*) Percentage of mosquitoes with melanized oocysts (*n*, number of experiments; 30 to 40 mosquitoes per experiment; day 14) infected with different *qc* mutant parasites (see *A* for mutant names). At least three replicates [except *Pbqc*(c): one experiment] were pooled for statistical analysis. Data are represented as mean ± SD. (*E*) Number of sg-sporozoites per mosquito (*n*, number of experiments; 60 to 80 mosquitoes per experiment) infected with *qc* mutants. Mean and SD [Δ*qc*: three to six experiments; WT: six experiments; *Pbqc*(c): one experiment; other mutants: two to four experiments]. **P < 0.005, *P < 0.05; ns, not significant [Mann–Whitney *U* test; significance relative to WT; *P* values: Δ*qc*1 0.0095, Δ*qc*2 0.004, Δ*qc*G 0.024, *Pfqc*(c) 0.262, *qc::cmyc* 0.191, and *qc^{CD}* 0.071]. (*F*) Examples of QC-null oocysts showing melanization of sporozoites inside or in the process of egress (*Left* and *Middle*); red arrows: melanized oocysts; blue arrows: WT-like oocysts. (*F, Inset*) WT oocyst with sporulation (day 14). (Scale bars, 20 μm.) (*F, Right*) Melanized QC-null hemocoel sporozoites (abdominal region; day 21). (Scale bar, 25 μm.) (*G*) Cluster of melanized (dark-colored, enlarged) sporozoites in the hemocoel of a QC-null–infected mosquito (day 21). (Scale bar, 10 μm.) (*H*) Bright-field and fluorescence images of salivary glands (day 21) from mosquitoes infected with WT (*Upper*) and QC-null parasites (*Lower*), expressing mCherry (*Right*). Melanized, mCherry-negative sporozoites cluster at the periphery of salivary glands. (Scale bars, 50 μm.) (*I*) Partially crushed salivary gland (day 21) of a QC-null–infected mosquito showing melanized (red arrowheads) and nonmelanized (blue arrowheads) sporozoites. (Scale bar, 10 μm.)

number of QC-null salivary gland sporozoites (sg-sporozoites) was significantly reduced compared with WT (Mann–Whitney $U$ test, $\Delta qc1$ $P = 0.0095$, $\Delta qc2$ $P = 0.0043$, and $\Delta qc\text{-}G$ $P = 0.0238$; Fig. 2E). However, most QC-null sporozoites inside salivary glands had a WT-like morphology, namely long and slender, without signs of melanization (Fig. 2I and *SI Appendix*, Fig. S2 *N* and *O*), suggesting that sporozoites escape the mosquito melanization response once they invade the salivary glands.

The melanization phenotype of *P. berghei* QC-null oocysts and sporozoites was analyzed in more detail. Scanning electron microscopy of QC-null oocysts and sporozoites with energy-dispersive X-ray (SEM-EDX) analysis revealed the presence of sulfur in the dark-colored parasites (Fig. 3), indicative of pheomelanin (23), a constituent of melanized ookinetes (24). The dark-colored material, hereinafter referred to as "melanin," was mainly located inside ruptured oocysts and on sporozoites. Distinct melanin deposition on the oocyst capsule was not observed (*SI Appendix*, Fig. S2 *K–O*). Transmission electron microscopy confirmed melanin deposition mainly inside oocysts, often surrounding sporozoites (*SI Appendix*, Fig. S3 *A* and *B*).

The motility of these QC-null sg-sporozoites and their infectivity of cultured hepatocytes were not significantly different from WT sg-sporozoites (*SI Appendix*, Fig. S3 *C–G*). These observations reveal the viability of QC-null sporozoites that invade salivary glands and indicate that the reduced sg-sporozoite numbers result from immune recognition and melanization of sporozoites while in transit to salivary glands. The melanization phenotype of QC-null parasites was rescued by genetic complementation through reintroduction of the *P. berghei* or the *P. falciparum* *qc* gene into the disrupted *qc* locus of *P. berghei* QC-null mutants (*SI Appendix*, Fig. S3 *H–N*). Complemented parasites showed WT-like oocyst and sporozoite development without signs of melanization, and sg-sporozoite numbers were also restored to WT numbers (Fig. 2 *A*, *B*, *D*, and *E* and *SI Appendix*, Fig. S3 *M* and *N* and Table S1).

The importance of QC activity to prevent melanization was further analyzed using a *P. berghei* mutant expressing a cyclase-dead QC containing two point mutations in the catalytic site (*SI Appendix*, Fig. S4 *A–D*). Similar to QC-null mutants, melanization was observed in this mutant with reduced sg-sporozoite numbers (Fig. 2 *A*, *B*, *D*, and *E* and *SI Appendix*, Fig. S4 *E* and *F* and Table S1), revealing that cyclase activity is critical to prevent sporozoite melanization.

We next investigated whether absence of QC activity in *P. falciparum* results in a melanization phenotype. Two independent *P. falciparum* mutants lacking the *qc* gene (*Pf∆qc1*, *Pf∆qc2*) were
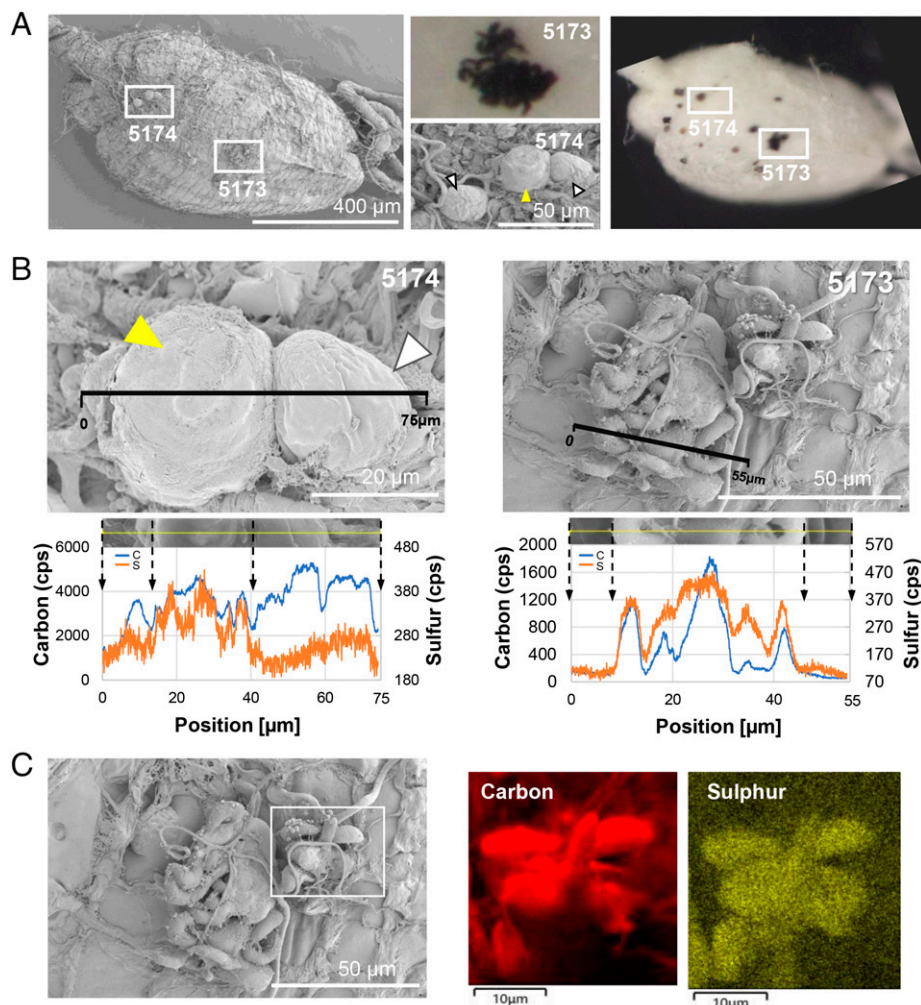


**Fig. 3.** SEM-EDX analysis of melanized and nonmelanized QC-null oocysts and sporozoites. (*A*) SEM (*Left*) and bright-field (*Right*) identification and selection of oocysts (5174) and sporozoites (5173) in a midgut of an *A. stephensi* mosquito infected with *Pb∆qc*1 (day 14). (*B*) EDX line scan of the elements carbon (blue) and sulfur (orange) together with SEM images (counts per second, CPS) showing the presence of sulfur in melanized oocysts (*Left*; dark-colored oocyst in 5174; *A*) and in melanized, dark-colored sporozoites (*Right*; 5173; *A*). Black lines represent EDX line scan positions. Yellow arrowheads indicate melanized black oocysts, and white arrowheads indicate nonmelanized oocysts (5174). Cluster of melanized sporozoites (5173). (*C*) EDX mapping analysis of carbon and sulfur together with an SEM image of melanized sporozoites (5173; *A*).

generated by CRISPR-Cas9 gene editing (*SI Appendix,* Fig. S4 *G–I*). These QC-null mutants showed similar asexual growth rate, gametocyte production (*SI Appendix,* Fig. S4 *J and K*), and numbers of oocysts and sg-sporozoites as WT parasites (Fig. 4 *A* and *B*). Melanization of oocysts and sporozoites also occurred in *P. falciparum* QC-null mutants, with melanized oocysts in 25 to 34% of infected mosquitoes (1 to 20 melanized oocysts per mosquito), whereas melanized parasites were absent in WT-infected mosquitoes (Fig. 4 *C–G*). Combined, we show that absence of QC results in melanization of oocysts and sporozoites of rodent and human malaria parasites.

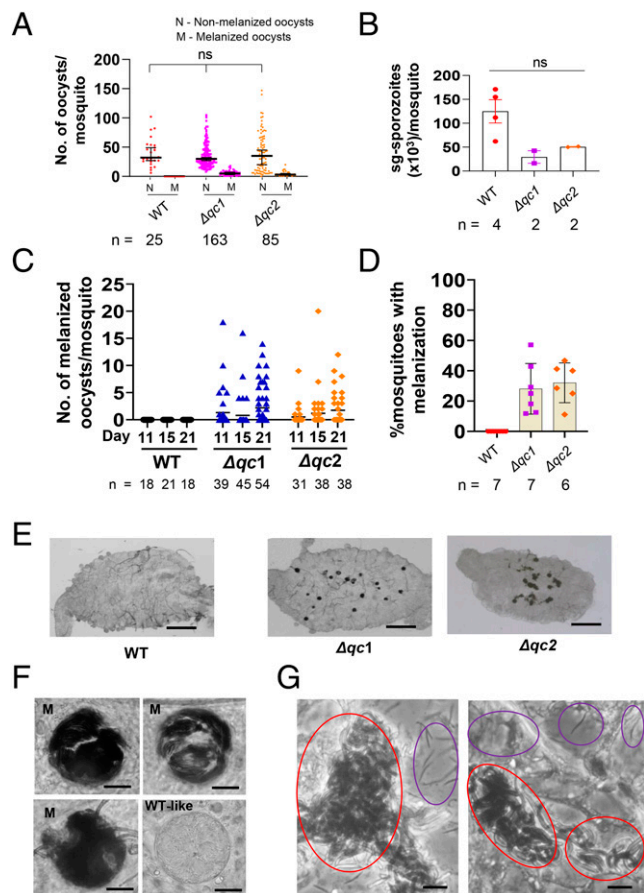**Fig. 4.** Melanization of oocysts and sporozoites of *P. falciparum* QC-null mutants. (*A*) Number of melanized and nonmelanized oocysts per mosquito in *A. stephensi* mosquitoes (*n*, number of mosquitoes) infected with QC-null mutants (Δ*qc*) or WT parasites. Error bars represent the median ± 95% CI (Δ*qc*: two experiments; WT: four experiments). ns, not significant (Mann–Whitney *U* test; statistical significance is shown relative to WT; *P* values: Δ*qc1* 0.333 and Δ*qc2* 0.531). (*B*) Number of sg-sporozoites per mosquito (*n*, number of experiments; 60 to 80 mosquitoes per experiment), infected with QC-null mutants (Δ*qc*) or WT parasites. Mean and SD [two experiments for QC-null mutants (Δ*qc*) and four experiments for WT]. ns, not significant (Mann–Whitney *U* test; statistical significance is shown relative to WT; *P* values: Δ*qc1* 0.133 and Δ*qc2* 0.133). (*C*) Number of melanized oocysts per individual mosquito on days 11, 15, and 21 after infection with QC-null mutants or WT parasites (*n*, number of mosquitoes). The horizontal bars indicate medians (two to four experiments). (*D*) Percentage of mosquitoes with melanized oocysts (*n*, number of experiments; 30 to 40 mosquitoes per experiment) at day 21 after infection with QC-null mutants or WT parasites. Data are represented as mean ± SD. (*E*) Melanized (dark-colored) oocysts in midguts of mosquitoes (day 11) infected with QC-null mutants. No melanized oocysts were observed in WT parasites. (Scale bars, 200 μm.) (*F*) Examples of (partly) melanized QC-null oocysts (M, day 15) showing melanization of sporozoites still inside or in the process of oocyst egress and an oocyst with typical features of WT sporozoite formation (WT-like). (Scale bars, 20 μm.) (*G*) Melanized (red circles) and nonmelanized, WT-like (purple circles) QC-null sporozoites obtained from a salivary gland (under a coverslip) isolated from an infected mosquito (day 21). (Scale bars, 10 μm.)

## Silencing of Mosquito Immune Responses Results in Reduced Melanization and Increased Sg-Sporozoite Numbers in QC-Null–Infected Mosquitoes.

TEP1 is a key effector of mosquito complement that targets ookinetes as they emerge from the midgut (15). A second TEP1-independent late-phase response, mediated by the STAT pathway (25) and hemocytes (26) targets the oocyst stage, while hemocyte-mediated phagocytosis of sporozoites has also been reported (27). Whereas substantial melanization has been documented in ookinetes (reviewed by ref. 12), extensive oocyst or sporozoite melanization has not been reported.

The melanization of QC-null parasites could result from either recognition of viable parasites as nonself by the immune system or as a general mechanism of disposal of aberrant/dead parasites (28) (reviewed by ref. 29). To examine whether abnormal/dead QC-expressing parasites would trigger a similar melanization response as QC-null parasites, we reanalyzed oocysts of four published *P. berghei* mutants that produce WT-like oocyst numbers but have severe defects in sporozoite formation [CSP- and ROM3-null mutants (30, 31)], egress from oocysts [CRMP4-null mutant (32)], or invasion of salivary glands [TRAP-null mutant (33)]. Despite these defects during sg-sporozoite formation, no melanization was observed (*SI Appendix,* Fig. S4 *L–R*), indicating that presence of aberrant parasites is not a general trigger for melanization. To further analyze whether the elimination of QC-null sporozoites involves mosquito hemocytes, we disrupted hemocyte function by systemic injection of polystyrene beads as described (34). Bead injection had no significant effect on the number of thorax sporozoites (including sg-sporozoites) in WT-infected mosquitoes (Fig. 5*A*) but significantly increased (2.6-fold) the number of QC-null thorax sporozoites, indicating that lack of QC activity results in active elimination of viable sporozoites that is mediated by hemocytes (Fig. 5*B*; Mann–Whitney *U* test, *P* < 0.01). The potential participation of the complement-like system in immune recognition of QC-null sporozoites was evaluated by silencing LRIM1, a stabilizer of TEP1 (35). Disrupting the complement system had no significant effect on the number of QC-null thorax sporozoites (Fig. 5*C*). In contrast, silencing the serine protease CLIPA8, a critical activator of melanization (28), reduced the percentage of QC-null–infected mosquitoes with melanized oocysts from 75 to 5% (Fig. 5*D*; $\chi^2$, *P* < 0.0001) and significantly increased the number of live thorax sporozoites (27.4-fold) (Fig. 5*E*; Mann–Whitney *U* test, *P* = 0.0001) and infection prevalence (66 to 90%; $\chi^2$, *P* < 0.01). Taken together, these findings demonstrate that QC-null sporozoites are detected as nonself and eliminated through melanization.

## QC-Null Oocysts Are Not Melanized When Sporozoite Formation or Egress Is Prevented.

The absence of melanized QC-null oocysts before day 10 p.i. and the lack of distinct deposition of melanin on the oocyst capsule may suggest that QC-null sporozoites, either still inside rupturing oocysts or after release into the hemocoel, are specifically recognized by the immune system. If this is the case, abolishing sporozoite formation inside QC-null oocysts or blocking egress of QC-null sporozoites would prevent oocyst melanization. To test this hypothesis, we deleted genes encoding proteins involved in sporozoite formation [CSP (30), ROM3 (31)] or in sporozoite egress [ECP1 (36), CRMP4 (32)] in h*dhfr*::y*fcu* selectable marker recycled *P. berghei* QC-null parasites [line *Pb*Δ*qc*1(-sm)] (*SI Appendix,* Fig. S5 *A–D*). These "double-knockout" QC-null mutants produced WT numbers of oocysts; however, melanized oocysts were completely absent (Fig. 6 *A* and *B* and *SI Appendix,* Fig. S5 *E–I*). In contrast, melanized oocysts/sporozoites were observed in 79% of mosquitoes infected
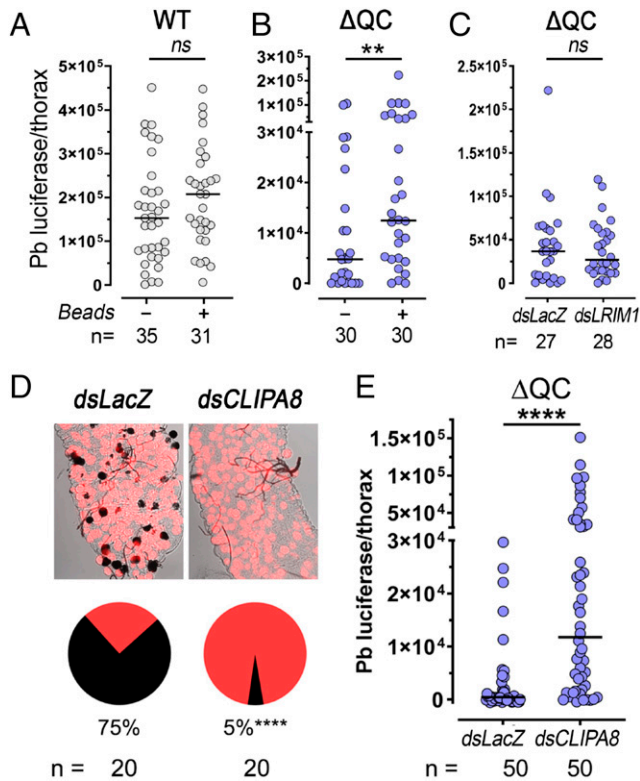
**Fig. 5.** Silencing of mosquito immune responses results in increased sporozoite numbers in salivary glands of mosquitoes infected with *P. berghei* QC-null mutants. (*A*) Sporozoite density (luciferase activity) in individual mosquito thoraces at day 23 p.i. after systemic injection of polystyrene beads into the thorax (day 12 p.i.) of mosquitoes infected with WT parasites (*n*, number of mosquitoes). ns, not significant (Mann–Whitney *U* test, *P* > 0.05). The horizontal bars indicate medians. (*B*) Sporozoite density (luciferase activity in individual mosquito thoraces; day 23 p.i.) after systemic injection of polystyrene beads into the thorax (day 12 p.i.) of QC-null (Δ*qc2*)–infected mosquitoes (*n*, number of mosquitoes). **\*\*P* < 0.01 (Mann–Whitney *U* test). The horizontal bars indicate medians. (*C*) Sporozoite density (luciferase activity in individual mosquito thoraces; day 23 p.i.) after injection of dsRNA for LRIM1 (ASTE000814) (dsLRIM1) or LacZ (dsLacZ; control) (day 12 p.i.) of QC-null mutant (Δ*qc2*)–infected mosquitoes (*n*, number of mosquitoes). ns, not significant (Mann–Whitney *U* test, *P* > 0.05). The horizontal bars indicate medians. (*D*) Representative midguts and percentage of mosquitoes with melanized (black) and nonmelanized (red) parasites (23 d p.i.) after injection of dsRNA for CLIPA8 (ASTE009395) (dsCLIPA8) or LacZ (dsLacZ; control) (day 12 p.i.) of QC-null mutant (Δ*qc2*)–infected mosquitoes (*n*, number of mosquitoes). **\*\*\*\*P* < 0.0001 ($\chi^2$ test). (*E*) Sporozoite density (luciferase activity in individual mosquito thoraces; day 23 p.i.) after injection of dsCLIPA8 or dsLacZ (control) (day 12 p.i.) of QC-null mutant (Δ*qc2*)–infected mosquitoes (*n*, number of mosquitoes). **\*\*\*\*P* < 0.0001 (Mann–Whitney *U* test). The horizontal bars indicate medians.

with a double-knockout QC-null mutant lacking the *trap* (33) gene (*SI Appendix*, Fig. S5*J*), in which sporozoites are released into the hemocoel but cannot invade the salivary glands (1 to 60 melanized oocysts per mosquito) (Fig. 6 *A* and *B* and *SI Appendix*, Fig. S5*J*). These observations confirm that melanization only occurs when QC-null oocysts rupture and sporozoites come in contact with mosquito hemolymph.

**Sporozoites Expressing the Circumsporozoite Surface Protein with a Mutated QC-Target Glutamine Are Recognized by the Mosquito Immune System.** Circumsporozoite protein (CSP) is the most abundant protein on the sporozoite surface (10, 11). We therefore hypothesized that CSP could be a prime target for immune recognition of QC-null parasites. We analyzed published proteomes for pGlu modification of CSP and identified multiple CSP peptides with pGlu at the N terminus. The majority (>90%) of these have pGlu modification of the

glutamine (Q) located in region 1 (R1) of CSP (*SI Appendix*, Fig. S5 *K* and *L*). This short, five–amino acid region (KLKQP) contains a proteolytic cleavage site (37, 38) and the glutamine is conserved across different *Plasmodium* species (Fig. 6*C*). CSP cleavage is known to occur at the sporozoite surface (39, 40) and this processing step is essential for host cell invasion (41). We hypothesized that the proteolytic cleavage site could be between the lysine and glutamine residues of R1, resulting in a glutamine at the new N terminus of processed CSP that can be modified. To establish whether CSP could be a target for immune recognition of the QC-null sporozoites, two independent *P. berghei* lines (*csp*^mut1,2) were generated that express a mutated CSP with glutamine in R1 replaced with alanine (Q92A), thereby preventing putative pGlu formation (Fig. 6*D* and *SI Appendix*, Fig. S5 *M–O*). Both *csp*^mut mutants produced similar numbers of oocysts as WT parasites (Fig. 6*E*). We confirmed proteolytic cleavage of CSP in both WT and *csp*^mut sg-sporozoites by Western analysis (Fig. 6*F*), indicating that the Q92A replacement did not affect CSP processing. The phenotype of *csp*^mut oocysts was similar to that of QC-null parasites, as no melanization was observed during the first 10 d p.i. whereas, at day 14 to 16 p.i., melanized oocysts were detected in 26 to 48% of *csp*^mut-infected mosquitoes (1 to 35 melanized oocysts per mosquito), mainly in ruptured oocysts (Fig. 6 *E*, *G*, and *H*). Clusters of melanized sporozoites were also found in the hemocoel of mosquitoes infected with *csp*^mut1 and *csp*^mut2 parasites (Fig. 6*I*). *csp*^mut sg-sporozoites also showed WT-like infectivity in cultured hepatocytes (*SI Appendix*, Fig. S5*P*). These observations demonstrate that the absence of the single glutamine residue in CSP R1 triggers immune recognition of viable/infective sporozoites in the mosquito hemocoel, resulting in parasite melanization. Combined, all our observations support the hypothesis that malaria parasites evade mosquito immune recognition by QC-mediated posttranslational modification of CSP.

## Discussion

Here, we present the functional characterization of a parasite QC and show that *Plasmodium* QC plays a role in sporozoite evasion of mosquito immune recognition. QC activity appears to be critical for survival of sporozoites emerging from oocysts or circulating in the hemocoel, but no other defects/phenotypes were observed in salivary gland sporozoites or in other developmental stages of QC-null parasites. *Plasmodium* evasion of mosquito immunity has been documented in the ookinete stage (42). Circulating hemocytes release microvesicles that promote local activation of TEP1 when they encounter the nitrated surface of *Anopheles gambiae* midgut cells undergoing apoptosis in response to ookinete invasion (14). The *P. falciparum* surface protein *Pfs*47 renders TEP1 activation ineffective by disrupting epithelial nitration in ookinete-invaded cells (43, 44). However, parasite factors implicated in immune evasion of sporozoites had not been reported. While TEP1-mediated lysis is key for immunity against ookinetes, here we show that the mosquito complement-like system does not mediate elimination of QC-null sporozoites, as silencing LRIM1 had no effect on sporozoite survival. We propose a mechanism of immune evasion (Fig. 7), in which QC modification of target proteins prevents melanization of sporozoites as they come in contact with mosquito hemolymph and increases the probability that they reach the salivary gland unharmed.

Sporozoite melanization is a major mechanism eliminating QC-null parasites, because disrupting melanization by silencing CLIPA8 greatly increased sporozoite survival. This also indicates
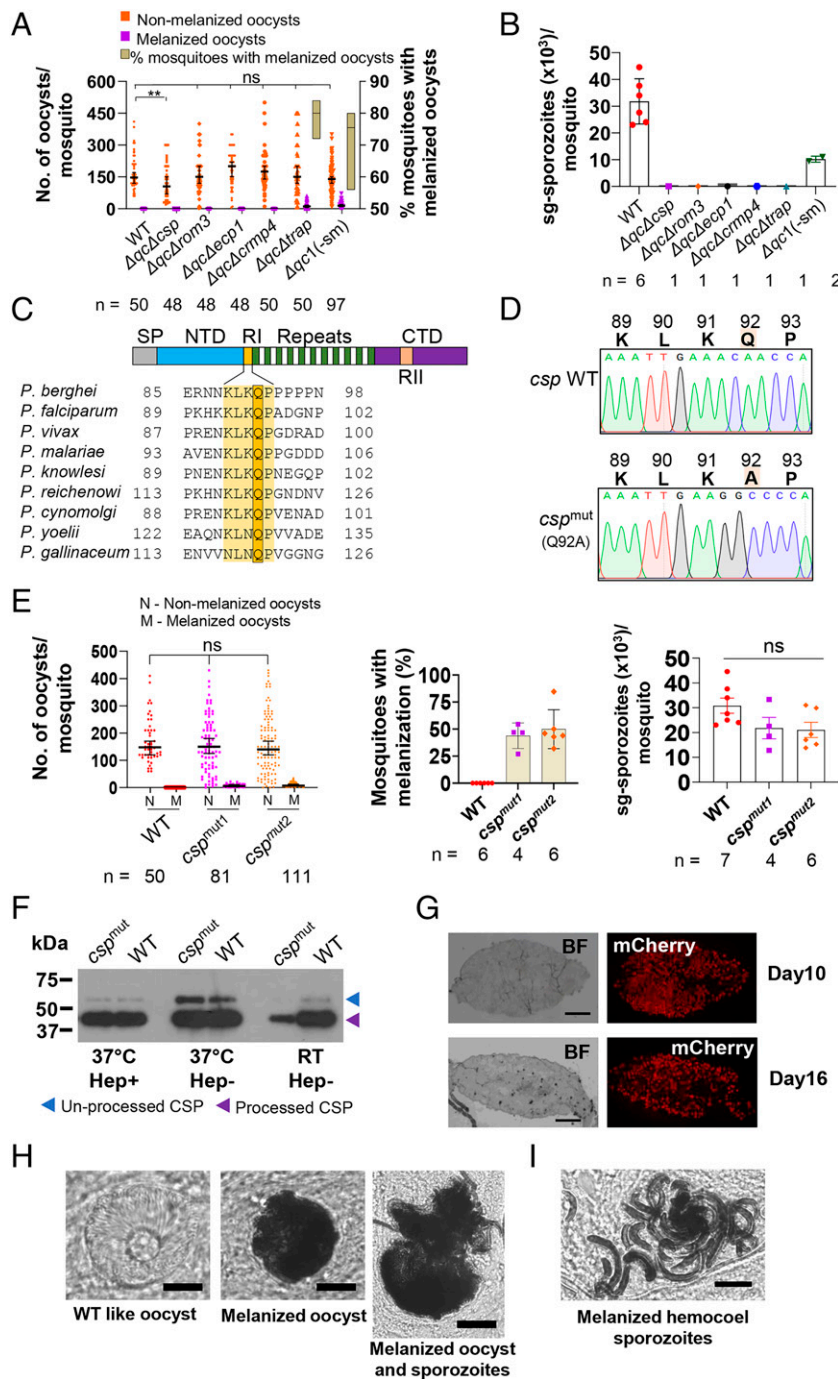
**A**

Non-melanized oocysts
Melanized oocysts
% mosquitoes with melanized oocysts

No. of oocysts/ mosquito — % mosquitoes with melanized oocysts

** ns

WT, $\Delta qc\Delta csp$, $\Delta qc\Delta rom3$, $\Delta qc\Delta ecp1$, $\Delta qc\Delta crmp4$, $\Delta qc\Delta trap$, $\Delta qc1(-sm)$

n = 50 48 48 48 50 50 97

**B**

sg-sporozoites ($\times 10^3$)/ mosquito

WT, $\Delta qc\Delta csp$, $\Delta qc\Delta rom3$, $\Delta qc\Delta ecp1$, $\Delta qc\Delta crmp4$, $\Delta qc\Delta trap$, $\Delta qc1(-sm)$

n = 6 1 1 1 1 1 2

**C**

SP  NTD  RI  Repeats  CTD
RII

| | 89 90 91 92 93 | |
| P. berghei | 85 | ERNNKLKQPPPPPN | 98 |
| P. falciparum | 89 | PKHKKLKQPADGNP | 102 |
| P. vivax | 87 | PRENKLKQPGDRAD | 100 |
| P. malariae | 93 | AVENKLKQPPGDDD | 106 |
| P. knowlesi | 89 | PNENKLKQPNEGQP | 102 |
| P. reichenowi | 113 | PKHNKLKQPGNDNV | 126 |
| P. cynomolgi | 88 | PRENKLKQPVENAD | 101 |
| P. yoelii | 122 | EAQNKLNQPVVADE | 135 |
| P. gallinaceum | 113 | ENVVNLNQPVGGNG | 126 |

**D**

89 90 91 92 93
K L K Q P

csp WT

89 90 91 92 93
K L K A P

csp^mut (Q92A)

**E**

N - Non-melanized oocysts
M - Melanized oocysts

No. of oocysts/ mosquito

ns

WT (N M), csp^mut1 (N M), csp^mut2 (N M)

n = 50 81 111

Mosquitoes with melanization (%)

WT, csp^mut1, csp^mut2

n = 6 4 6

sg-sporozoites ($\times 10^3$)/ mosquito

ns

WT, csp^mut1, csp^mut2

n = 7 4 6

**F**

kDa

csp^mut WT  csp^mut WT  csp^mut WT

75—
50—
37—

37°C Hep+  37°C Hep−  RT Hep−

◀ Un-processed CSP  ◀ Processed CSP

**G**

BF  mCherry  Day10

BF  mCherry  Day16

**H**

WT like oocyst

Melanized oocyst

Melanized oocyst and sporozoites

**I**

Melanized hemocoel sporozoites

**Fig. 6.** Absence of melanization of QC-null oocysts in the absence of sporozoite egress, and melanization of oocysts and sporozoites that express CSP with a mutated QC-target glutamine. (A) Number of melanized and nonmelanized oocysts per mosquito (median ± 95% CI; n = 40 to 50) infected with a QC-null mutant [Δqc1(-sm)], WT and QC-null mutants $\Delta qc\Delta csp$, $\Delta qc\Delta rom3$ (no sporozoite formation), $\Delta qc\Delta ecp1$, $\Delta qc\Delta crmp4$ (no sporozoite egress), and $\Delta qc\Delta trap$ (sporozoite egress). n, number of mosquitoes. y axis (Right): percentage of mosquitoes with melanized oocysts [three experiments for all mutants except for Δqc1(-sm), n = 4]. ns, not significant [Mann–Whitney U test; significance relative to WT; P values: $\Delta qc\Delta csp$ 0.003, $\Delta qc\Delta rom3$ 0.968, $\Delta qc\Delta ecp1$ 0.184, $\Delta qc\Delta crmp4$ 0.216, $\Delta qc\Delta trap$ 0.895, and $\Delta qc$(-sm) 0.075]. (B) Number of sg-sporozoites per mosquito infected with mutants as shown (Left) (n, number of experiments; 60 to 80 mosquitoes per experiment). Data are represented as mean ± SD. ns, not significant [Mann–Whitney U test; significance relative to WT; P value: Δqc(-sm) 0.071]. (C) Schematic showing different regions of CSP. Yellow: region 1 (RI). Dark yellow box: the conserved glutamine in R1 (KLKQP). R1 is highly conserved and contains the cleavage site (41). CTD, C-terminal domain; NTD, N-terminal domain; SP, signal peptide. (D) Sanger-sequence DNA chromatograms of the PCR fragment of P. berghei CSP RI amplified from WT and csp^mut genomic DNA, confirming the replacement of glutamine with alanine (Q92A; highlighted) in csp^mut. (E, Left) Number of melanized and nonmelanized oocysts per mosquito in A. stephensi mosquitoes (n, number of mosquitoes) infected with CSP Q92A mutants (CSP^mut1 and CSP^mut2) or WT parasites. Error bars represent the median ± 95% CI (four to six experiments). ns, not significant (Mann–Whitney U test; statistical significance is shown relative to WT; P values: csp^mut1 0.439 and csp^mut2 0.264). (E, Middle) Percentage of mosquitoes with melanized oocysts (n, number of experiments; 30 to 40 mosquitoes per experiment; day 16) infected with csp^mut. No melanized oocysts in WT-infected mosquitoes. Data are represented as mean ± SD. (E, Right) Number of sg-sporozoites per mosquito (day 21; n, number of experiments; 60 to 80 mosquitoes per experiment) infected with WT, csp^mut1, and csp^mut2. Data are represented as mean ± SD (n, number of experiments). ns, not significant (Mann–Whitney U test; significance relative to WT; P values: csp^mut1 0.073 and csp^mut2 0.073). (F) Western analysis of sporozoite lysates showing CSP expression/processing in WT and csp^mut, expressing mutated CSP (Q92A), using antibody 3D11, recognizing CSP repeats. Processing results in a full-length (55 kDa) and a processed form (45 kDa) (39, 48). WT and csp^mut sporozoites incubated with or without heparin at 37 °C or room temperature (RT; 10 min) as CSP also undergoes processing when in contact with heparan sulfate proteoglycans (21). (G) Midguts of mosquitoes with mCherry-expressing csp^mut oocysts, showing melanized (dark-colored) oocysts. (Scale bars, 200 μm.) (H) Bright-field light-microscope images of csp^mut oocysts (day 21) showing WT-like (WT-ooc) and melanized oocysts. (H, Right) Melanized sporozoites during egress. (Scale bars, 20 μm.) (I) Melanized csp^mut sporozoites in the hemocoel (abdominal region; day 21). (Scale bar, 10 μm.)
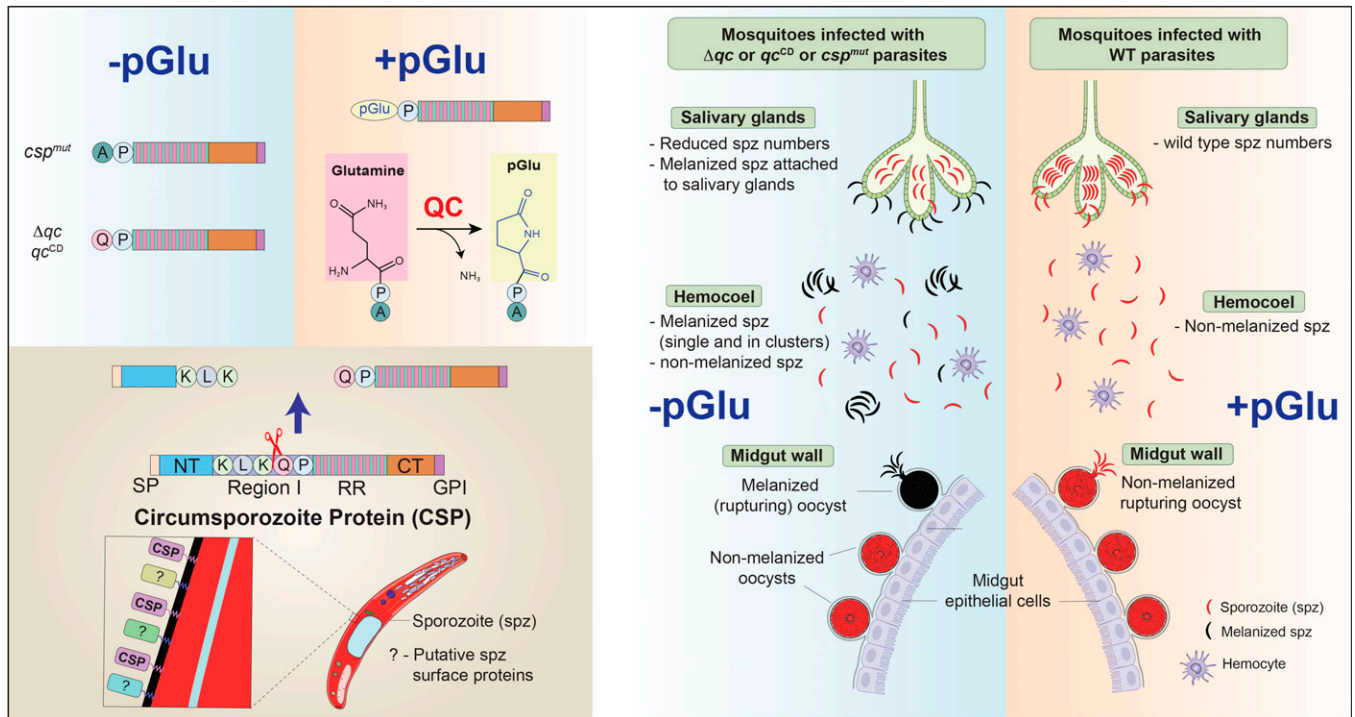
**Fig. 7.** Proposed model of immune evasion of WT oocysts and sporozoites by posttranslational modification of proteins by QC. A mechanism of immune evasion by *Plasmodium* in the mosquito host is proposed in which QC modification of *Plasmodium*-target proteins prevents melanization of sporozoites (spz) as they come in contact with mosquito hemolymph. QCs posttranslationally modify proteins with N-terminal glutamine or glutamic acid to a cyclic pyroglutamic acid. Sporozoites and rupturing oocysts lacking QC activity (Δ*qc*, *qc*^CD) or expressing CSP with a mutated glutamine (in R1, *csp*^mut) are recognized and melanized (indicated as black oocyst and sporozoites). Sporozoites of Δ*qc*, *qc*^CD, and *csp*^mut are also melanized in the hemocoel. Sporozoites that escape melanization and successfully invade the salivary gland are protected from mosquito immune attack. Sporozoite melanization is a major mechanism eliminating Δ*qc* sporozoites, because disrupting melanization by silencing CLIPA8 significantly increases the number of viable Δ*qc* sporozoites. This indicates that sporozoite melanization is not activated in response to parasites that are already dead or irreversibly damaged. Mutating a single QC-target glutamine of CSP, the major sporozoite surface protein, also results in melanization of sporozoites. pGlu formation at this glutamine of WT sporozoites requires processing of CSP. CSP cleavage in R1 occurs at the sporozoite surface. We propose a working model in which proteolytic cleavage of CSP in R1 (KLK↓QP), between lysine and glutamine, generates an N-terminal glutamine that is posttranslationally modified to pGlu by the enzymatic activity of QC, and this posttranslational modification increases the probability that sporozoites will reach the salivary gland unharmed. CT, C-terminal fragment; NT, N-terminal fragment; RR, repeat region; SP, signal peptide (amino acids in R1 are shown as single-letter codes).

that sporozoite melanization is not activated in response to parasites that are already dead or irreversibly damaged. Consistent with our results, previous studies found that, although a majority of injected WT sporozoites (80 to 90%) are eliminated and lysed before they invade the salivary glands, only a small proportion of WT sporozoites are eliminated by phagocytosis or melanization (27, 45). *Plasmodium* ookinete melanization has been reported as a mechanism to dispose of dead or irreversibly damaged ookinetes, because disrupting melanization of ookinetes in the refractory *A. gambiae* L35 strain does not increase parasite survival (28). In contrast, our results show that melanization can eliminate viable sporozoites in the absence of QC activity. All our results indicate that melanization of QC-null parasites occurs when oocysts rupture and sporozoites come in contact with mosquito hemolymph. Indeed, melanization of QC-null mutants is not observed in early oocyst stages, in mature oocysts before rupture, or in double-knockout QC-null oocysts that never rupture. The observation that the number of melanized oocysts does not increase between 14 and 21 d p.i. was unexpected. It may reflect how quickly oocysts are melanized as they begin to rupture. For example, one can envision that hemolymph levels of tyrosine, a substrate essential for melanization, are probably higher 10 to 14 d p.i. and oocysts may be melanized very quickly as soon as they begin to rupture. Some sporozoites emerging from oocysts that rupture later may be able to escape into the hemolymph before they are melanized. Some of these sporozoites are melanized after they emerge, on the surface of the salivary gland

(as in Fig. 2*H*) or other organs. When oocyst numbers are high, we observe that many oocysts never rupture, even 21 d p.i., both in WT and QC-mutant parasites. Those oocysts are not melanized in QC-mutant parasites.

Our observation that bead injection increases parasite survival shows that hemocytes are involved in the elimination of QC-null sporozoites. However, one must consider that the number of circulating sporozoites is significantly lower in QC-null parasites than in WT, as bundles of melanized sporozoites are often observed before they emerge from ruptured oocysts or are attached to the hemocoel surface. It is thus possible that the higher efficiency of phagocytosis in QC-null sporozoites by hemocytes could be indirect and due, at least in part, to the reduced number of parasites circulating in the hemocoel. If this is the case, one would expect that phagocytosis in QC-null parasites would be even more effective in natural infections in which only a handful of oocysts are present.

We provide direct evidence that QC-mediated modification of *P. berghei* CSP plays a role in escaping immune recognition. This surface protein has multiple essential functions during key infection processes in both the mosquito and vertebrate host (10, 11, 46) and is a principal target for various malaria vaccination approaches (10, 11, 47). pGlu formation at the mutated glutamine requires processing of CSP. CSP cleavage in R1 occurs at the sporozoite surface (39, 40, 48) and QC has been identified in sporozoite surface proteomes (21, 49, 50). We propose a working model (Fig. 7) in which proteolytic cleavage

in R1 of CSP (KLK↓QP) on the surface of sporozoites, between lysine (K) and glutamine (Q), generates an N-terminal glutamine that is posttranslationally modified to pGlu by *Plasmodium* QC. There has been controversy as to whether R1 of CSP is already processed in sg-sporozoites (36, 39, 40, 51) or whether cleavage takes place later on, when sporozoites come in contact with the surface of hepatocytes (41). However, because CSP is constantly shed from the surface of sporozoites (52, 53) and sporozoites can remain for several days within the mosquito salivary gland, one can envision that most CSP molecules present on the surface of sporozoites emerging from oocysts may have been replaced with new CSP by the time sporozoites are injected into the skin of the vertebrate host. Thus, it is possible that processing of CSP R1 is required at multiple stages, and there may be differences in CSP processing between sporozoites present in the mosquito and in the vertebrate host. In two studies in which the complete R1 region of CSP was removed in *P. berghei* mutants, cleavage of the N-terminal region of CSP no longer took place, and the number of parasites that reached the salivary gland was reduced (37, 54). However, no melanization of the mutated oocysts or sporozoites was reported, suggesting that unprocessed CSP does not activate melanization, while CSP that has been processed by cleavage in R1 acquires a conformation that activates melanization in the mosquito, unless the N-terminal Q that is generated is modified to pGlu by QC. The increased melanization of *csp*^mut parasites in which a single amino acid (Q in the R1 region) of CSP was mutated shows that CSP is an important target of QC. Whether CSP is the only target protein for QC-mediated modification in sporozoites to evade immune recognition is unknown. We did not observe any phenotypes in other life cycle stages of QC-null parasites that were different from WT. Moreover, sg-sporozoites of the QC-null mutants that escaped melanization showed a WT-like motility and infectivity to hepatocytes, indicating that lack of QC does not affect other sporozoite proteins involved in motility and invasion. However, the lower percentage of mosquitoes with melanized *csp*^mut oocysts, and fewer melanized *csp*^mut oocysts per mosquito compared with QC-null–infected mosquitoes, suggests that there are probably other targets of QC besides CSP.

Our studies reveal a mechanism of immune evasion of malaria parasites in the mosquito, by QC modification of target proteins, including CSP. Human QCs posttranslationally modify multiple proteins involved in different processes, including immune evasion by malignant cells (7, 8). In human cells, QC activity modifies the N-terminal glutamine of CD47 to pGlu (7). This N-terminal modification is essential for CD47 binding to SIRPα, an inhibitory receptor primarily expressed in myeloid cells. Thus, cancer cells evade immunity by overexpressing CD47, which is modified by QC, and suppresses myeloid cells by interacting with SIRPα (55). Combined, our findings indicate that QC-mediated posttranslational protein modification is an ancient immune evasion strategy, shared by evolutionarily distant eukaryotes. We show that it facilitates malaria transmission by enhancing sporozoite survival during their transit to the mosquito salivary gland. Understanding how the malaria parasite evades mosquito immunity could open the possibility to designing novel strategies to disrupt disease transmission. We provide direct evidence that type I QC, an enzyme present in bacteria, plants, and parasites, mediates immune evasion. Interestingly several other pathogenic organisms, such as *Toxoplasma gondi* and *Yersinia pestis*, also have type I QC genes (3). Our observations beg the question of whether these, or other pathogens, use a similar immune evasion strategy in their insect vectors, or in their vertebrate hosts. The importance of QC modifications for infectivity of sporozoites in vertebrates, as they transit through the skin, the circulatory system, and the liver, also remains to be determined.

## Materials and Methods

**Experimental Animals: Leiden University Medical Center.** All animal experiments were granted a license by competent authority after advise on ethical evaluation by the Animal Experiments Committee Leiden (AVD1160020171625). All experiments were performed in accordance with the Experiments on Animals Act (Wod, 2014), the applicable legislation in The Netherlands in accordance with European guidelines (EU directive no. 2010/63/EU). All experiments were executed in a licensed establishment for experimental animals (Leiden University Medical Center; LUMC). Mice were housed in ventilated cages furnished with autoclaved aspen woodchips, fun tunnel, wood chew block, and nestlets (at 21 ± 2 °C; 12-h light-dark cycle; relative humidity of 55 ± 10%) and fed commercially prepared autoclaved dry rodent diet pellets and provided with water, both available ad libitum. Female OF1 mice (6- to 7-wk-old, Charles River Laboratories) were used (see *SI Appendix* for additional information).

Mosquitoes from a colony of *A. stephensi* (line Nijmegen SDA500) were used. Larval stages were reared in water trays (at 28 ± 1 °C; relative humidity 80%). Adult females were transferred to incubators at 28 ± 0.2 °C (relative humidity 80%) and fed a 5% filter-sterilized glucose solution. For the transmission experiments, 3- to 5-d-old mosquitoes were used. Following infection, the *P. berghei*– and *P. falciparum*–infected mosquitoes were maintained at 21 and 28 °C, respectively, at 80% relative humidity.

**Experimental Animals: NIH.** Female BALB/c mice (6- to 7-wk-old from Charles River Laboratories) were used following approved NIH animal protocol LMVR-5. *A. stephensi* Nijmegen mosquitoes were reared under standard conditions at 27 °C and 80% humidity (12-h light–dark cycle).

**Parasites.** Parasites of the transgenic reference line 1868cl1 were used as "WT" *P. berghei* (*Pb*) ANKA parasite. Parasites of this reference ANKA line express mCherry and luciferase under the constitutive *hsp70* and *eef1a* promotors, respectively (RMgm-1320, http://www.pberghei.eu) (56). The following *Pb* ANKA mutant lines were used: Δ*rom3* (430cl1; mutant RMgm-178, http://www.pberghei.eu) (31), Δ*crmp4* (376cl1; RMgm-585, http://www.pberghei.eu) (32), Δ*trap* (2564cl3; RMgm-4680, http://www.pberghei.eu) (33), and Δ*csp* (3065cl1; RMgm-4681, http://www.pberghei.eu) (30). Parasites of Δ*csp* and Δ*rom3* (*csp*, PBANKA_0403200; *rom3*, PBANKA_0702700) lack signs of sporozoite formation/maturation inside oocysts (30, 31). Parasites of Δ*crmp4* (*crmp4*, PBANKA_1300800) form sporozoites that are unable to egress from the mature oocysts (32). Parasites of Δ*trap* (*trap*, PBANKA_1349800) form sporozoites inside oocysts that egress from the oocysts but are unable to invade the salivary glands (33). In addition, mutant line *Pb*Δ*csp*-GIMO parasites (https://www.pberghei.eu/index.php?rmgm=4681) were used. In the genome of parasites of this line the *csp* open reading frame has been replaced by the h*dhfr::yfcu* selectable marker. Parasites of this line lack sporozoite formation/maturation inside oocysts. *P. falciparum* NF54 strain parasites (57) were used as WT *P. falciparum* parasites (WT Pf) (see *SI Appendix* for additional information).

**Bioinformatic Analyses.** Gene and amino acid sequences of QC (QPCT, putative) from *Plasmodium* species were retrieved from PlasmoDB v.46 (http://www.plasmodb.org). Similarity and identity between QC of *Plasmodium* species were calculated using MatGAT (58). The three-dimensional structure of *Pf*QC (PF3D7_1446900) was generated against the resolved QC structures from *C. papaya* (Protein Data Bank [PDB] ID code 2IWA) and *Zymomonas mobilis* (PDB ID code 3NOL) using the I-TASSER structure prediction tool (59, 60). PyMOL (https://pymol.org/2/) was used to visualize 3D protein structure. Secondary structure of *Pf*QC was aligned with the QCs from *C. papaya* (PDB ID code 2IWA) (20), *Z. mobilis* (PDB ID code 3NOL) (18), *Xanthomonas campestris* (PDB ID code 3MBR) (19), and *Myxococcus xanthus* (PDB ID code 3NOK) (18) (see *SI Appendix* for additional information).

**Enzymatic Characterization of *Plasmodium* QC.** A two-step cyclase activity assay was performed using recombinant WT *Pf*QC and a cyclase-dead *Pf*QC,

containing two mutated amino acid residues (F107A and Q109A) in the active site (*Pf*QC$^{CD}$) (see *SI Appendix* for additional information).

**Generation and Genotyping of Different *P. berghei* QC-Null Mutants.** To generate QC-null mutants, the *Pbqc* gene (PBANKA_1310700) was deleted by standard methods of transfection (61) using the *Not*I-linearized gene-deletion plasmid *Pb*GEM-342996, obtained from PlasmoGEM (https://plasmogem.umu.se/pbgem/) (62, 63). This construct contains the positive–negative h*dhfr*::*yfcu* selectable marker cassette. Transfection of parasites (line 1868cl1) in two independent experiments, followed by pyrimethamine selection and subsequent cloning of the parasites (61), resulted in selection of two gene-deletion mutants, *Pb*Δ*qc*1 (line 2930cl1) and *Pb*Δ*qc*2 (line 2931cl1). Correct integration of the constructs and deletion of the *qc* gene were verified by Southern analyses of pulsed-field gel (PFG)–separated chromosomes and diagnostic PCR analysis (61). PFG-separated chromosomes were hybridized with a mixture of two probes: a probe recognizing the h*dhfr* gene and a control probe recognizing gene PBANKA_0508000 on chromosome 5 (64). PCR primers for genotyping are listed in *SI Appendix*, Table S2 (see *SI Appendix* for additional information).

**Generation and Genotyping of *P. falciparum* QC-Null Mutants.** The *Pfqc* (PF3D7_1446900) gene was deleted in WT *Pf* parasites by standard methods of CRISPR-Cas9 transfection (65) using two different single-guide RNAs in combination with donor DNA (see *SI Appendix* for additional information).

**Phenotype Analysis of *P. berghei* QC Mutants.** The in vivo multiplication rate of asexual blood stages was determined during the cloning procedure of the different QC mutants (66). In vitro cultivation of ookinetes, using gametocyte-enriched infected blood, was performed as described (67). In brief, enriched gametocytes were collected from phenylhydrazine-treated mice and mixed with standard ookinete culture medium. The cultures were incubated at 21 to 22 °C for 18 to 24 h. Ookinete conversion/fertilization rate was calculated by counting unfertilized female gametes and mature ookinete stages in Giemsa-stained smears 18 to 24 h after in vitro gametocyte activation (see *SI Appendix* for additional information).

**Phenotype Analysis of *P. falciparum* Mutants.** The growth rate of asexual blood stages of *P. falciparum* parasites was determined in 10-mL cultures maintained in the semiautomated culture system as described (68). Gametocyte production and exflagellation were quantified in gametocyte cultures as described (65).

For mosquito transmission experiments, female *A. stephensi* mosquitoes were fed on gametocyte cultures using the standard membrane feeding assay (65, 69). Oocyst and sporozoite production were monitored in infected mosquitoes as described (65, 70). Oocysts were analyzed on day 11, 15, and 21 p.i. and the percentage of melanized oocysts was determined by analyzing manually dissected midguts using a Leica MZ16 FA stereofluorescence microscope. The midguts were imaged with a Leica MZ camera at 10× magnification using Leica LAS X software. Individual melanized and WT-like oocysts were observed under a Leica DM2500 light microscope and documented at 100× using a Leica DC500 digital camera using Leica LAS X software. Sg-sporozoite numbers were analyzed in infected mosquitoes at day 18 to 21 p.i. For counting sporozoites, salivary glands from 30 to 60 mosquitoes were dissected and homogenized using a grinder in 100 μL RPMI-1640 medium (pH 7.2) and sporozoites were analyzed in a Bürker cell counter using phase-contrast microscopy (65).

**Disruption of the Mosquito Immune System.** Mosquito hemocyte depletion was carried out as previously described (14). Briefly, *A. stephensi* mosquitoes received an injection of 200,000 1-μm-diameter polystyrene beads (FluoSpheres, Life Technologies) in 138 nL water using a Nanoject injector (Drummond

Scientific). Polystyrene beads were washed extensively with water before injecting mosquitoes in the side of the thorax at 12 d p.i. Water injection was used as a control.

The abundance of sporozoites was determined by measuring luciferase activity in the thorax of mosquitoes infected with *P. berghei* WT and mutant parasites that express luciferase constitutively.

Mosquito thoraces were collected at 23 d p.i. in individual tubes, frozen in dry ice immediately, and stored at −30 °C until processing. The Luciferase Assay System Kit (Promega) was used to measure the luciferase activity in sporozoite samples following the manufacturer's instructions (see *SI Appendix* for additional information).

**Statistical Analysis.** Data were analyzed using Prism v.7 or above (GraphPad Software). Statistical analyses were performed using the nonparametric unpaired *t* test following Mann–Whitney *U* test, *t* test for QC activity, and sporozoite gliding motility assays, and $\chi^2$ test (one-sided) for analyzing CLIP8 double-stranded RNA (dsRNA)–mediated inhibition experiments.

**Data, Materials, and Software Availability.** All study data are included in the article and/or *SI Appendix*.

Author affiliations: [a]Malaria Research Group, Department of Parasitology, Leiden University Medical Center, Leiden, 2333 ZA, The Netherlands; [b]Laboratory of Malaria and Vector Research, National Institute of Allergy and Infectious Diseases, NIH, Rockville, MD, 20852; [c]Department of Parasitology, National Institute of Infectious Diseases, Shinjuku-ku, Tokyo 162-8640, Japan; [d]Interventional Molecular Imaging Laboratory, Department of Radiology, Leiden University Medical Center, Leiden, 2333 ZA, The Netherlands; [e]Oncode Institute, Leiden University Medical Center, Leiden, 2333 ZC, The Netherlands; [f]Department of Cell and Chemical Biology, Leiden University Medical Center, Leiden, 2333 ZC, The Netherlands; [g]Department of Life Sciences, Imperial College London, London, SW7 2AZ, United Kingdom; [h]Laboratory of Morphology and Image Analysis, Research Support Center, Juntendo University Graduate School of Medicine, Bunkyo, Tokyo 113-8421, Japan; [i]Department of Pathology, National Institute of Infectious Diseases, Shinjukuku, Tokyo 162-8640, Japan; [j]Center for Proteomics and Metabolomics, Leiden University Medical Center, Leiden, 2333 ZA, The Netherlands; and [k]Department of Dermatology, Leiden University Medical Center, Leiden, 2300 RC, The Netherlands

Author contributions: S.K.K., A.M.-C., M.C., C.B.-M., F.A.S., and C.J.J. designed research; S.K.K., A.M.-C., T. Araki, F.J.A.-v.G., J.R., S.C.-M., H.J.K., S.B., C.d.K., R.W., N.R., A.F.E.H., R.Q.K., M.C., S.K., H.H., H.K., T. Annoura, P.J.H., B.M.F.-F., F.A.S., and C.J.J. performed research; S.K.K., A.M.-C., C.B.-M., F.A.S., and C.J.J. analyzed data; and S.K.K., A.M.-C., T. Araki, T. Annoura, P.J.H., C.B.-M., F.A.S., and C.J.J. wrote the paper.

1. R. Wintjens *et al.*, Crystal structure of papaya glutaminyl cyclase, an archetype for plant and bacterial glutaminyl cyclases. *J. Mol. Biol.* **357**, 457–470 (2006).
2. R. E. Booth, S. C. Lovell, S. A. Misquitta, R. C. Bateman Jr., Human glutaminyl cyclase and bacterial zinc aminopeptidase share a common fold and active site. *BMC Biol.* **2**, 2 (2004).
3. S. Schilling, C. Wasternack, H. U. Demuth, Glutaminyl cyclases from animals and plants: A case of functionally convergent protein evolution. *Biol. Chem.* **389**, 983–991 (2008).
4. D. K. Vijayan, K. Y. J. Zhang, Human glutaminyl cyclase: Structure, function, inhibitors and involvement in Alzheimer's disease. *Pharmacol. Res.* **147**, 104342 (2019).
5. T. C. Saido *et al.*, Dominant and differential deposition of distinct beta-amyloid peptide species, A beta N3(pE), in senile plaques. *Neuron* **14**, 457–466 (1995).
6. T. L. Tekirian, A. Y. Yang, C. Glabe, J. W. Geddes, Toxicity of pyroglutaminated amyloid beta-peptides 3(pE)-40 and -42 is similar to that of A beta1-40 and -42. *J. Neurochem.* **73**, 1584–1589 (1999).

7. M. E. W. Logtenberg *et al.*, Glutaminyl cyclase is an enzymatic modifier of the CD47- SIRPα axis and a target for cancer immunotherapy. *Nat. Med.* **25**, 612–619 (2019).
8. Z. Wu *et al.*, Identification of glutaminyl cyclase isoenzyme isoQC as a regulator of SIRPα-CD47 axis. *Cell Res.* **29**, 502–505 (2019).
9. D. Vlachou, T. Schlegelmilch, E. Runn, A. Mendes, F. C. Kafatos, The developmental migration of *Plasmodium* in mosquitoes. *Curr. Opin. Genet. Dev.* **16**, 384–391 (2006).
10. K. Dundas, M. J. Shears, P. Sinnis, G. J. Wright, Important extracellular interactions between *Plasmodium* sporozoites and host cells required for infection. *Trends Parasitol.* **35**, 129–139 (2019).
11. F. Frischknecht, K. Matuschewski, *Plasmodium* sporozoite biology. *Cold Spring Harb. Perspect. Med.* **7**, a025478 (2017).
12. A. M. Clayton, Y. Dong, G. Dimopoulos, The *Anopheles* innate immune system in the defense against malaria infection. *J. Innate Immun.* **6**, 169–181 (2014).

13. G. d. A. Oliveira, J. Lieberman, C. Barillas-Mury, Epithelial nitration by a peroxidase/NOX5 system mediates mosquito antiplasmodial immunity. *Science* **335**, 856–859 (2012).

14. J. C. Castillo, A. B. B. Ferreira, N. Trisnadi, C. Barillas-Mury, Activation of mosquito complement antiplasmodial response requires cellular immunity. *Sci. Immunol.* **2**, eaal1505 (2017).

15. S. Blandin et al., Complement-like protein TEP1 is a determinant of vectorial capacity in the malaria vector *Anopheles gambiae. Cell* **116**, 661–670 (2004).

16. A. Kumar et al., Mosquito innate immunity. *Insects* **9**, 95 (2018).

17. M. A. Osta, G. K. Christophides, F. C. Kafatos, Effects of mosquito genes on *Plasmodium* development. *Science* **303**, 2030–2032 (2004).

18. D. R. Carrillo et al., Kinetic and structural characterization of bacterial glutaminyl cyclases from *Zymomonas mobilis* and *Myxococcus xanthus. Biol. Chem.* **391**, 1419–1428 (2010).

19. W. L. Huang et al., Crystal structure and functional analysis of the glutaminyl cyclase from *Xanthomonas campestris. J. Mol. Biol.* **401**, 374–388 (2010).

20. T. Guevara et al., Papaya glutamine cyclotransferase shows a singular five-fold beta-propeller architecture that suggests a novel reaction mechanism. *Biol. Chem.* **387**, 1479–1486 (2006).

21. K. E. Swearingen et al., Interrogating the *Plasmodium* sporozoite surface: Identification of surface-exposed proteins and demonstration of glycosylation on CSP and TRAP by mass spectrometry-based proteomics. *PLoS Pathog.* **12**, e1005606 (2016).

22. R. Tewari, D. Rathore, A. Crisanti, Motility and infectivity of *Plasmodium berghei* sporozoites expressing avian *Plasmodium gallinaceum* circumsporozoite protein. *Cell. Microbiol.* **7**, 699–707 (2005).

23. M. M. A. Whitten, C. J. Coates, Re-evaluation of insect melanogenesis research: Views from the dark side. *Pigment Cell Melanoma Res.* **30**, 386–401 (2017).

24. E. Camacho et al., Analysis of melanotic *Plasmodium* spp. capsules in mosquitoes reveal eumelanin-pheomelanin composition and identify AgMesh as a modulator of parasite infection. bioRxiv [Preprint] (2021). https://doi.org/10.1101/2021.05.07.443077 (Accessed 9 January 2022).

25. L. Gupta et al., The STAT pathway mediates late-phase immunity against *Plasmodium* in the mosquito *Anopheles gambiae. Cell Host Microbe* **5**, 498–507 (2009).

26. R. C. Smith, C. Barillas-Mury, M. Jacobs-Lorena, Hemocyte differentiation mediates the mosquito late-phase immune response against *Plasmodium* in *Anopheles gambiae. Proc. Natl. Acad. Sci. U.S.A.* **112**, E3412–E3420 (2015).

27. J. F. Hillyer, S. L. Schmidt, B. M. Christensen, Rapid phagocytosis and melanization of bacteria and *Plasmodium* sporozoites by hemocytes of the mosquito *Aedes aegypti. J. Parasitol.* **89**, 62–69 (2003).

28. J. Volz, H. M. Müller, A. Zdanowicz, F. C. Kafatos, M. A. Osta, A genetic module regulates the melanization response of *Anopheles* to *Plasmodium. Cell. Microbiol.* **8**, 1392–1405 (2006).

29. C. Barillas-Mury, CLIP proteases and *Plasmodium* melanization in *Anopheles gambiae. Trends Parasitol.* **23**, 297–299 (2007).

30. R. Ménard et al., Circumsporozoite protein is required for development of malaria sporozoites in mosquitoes. *Nature* **385**, 336–340 (1997).

31. J. W. Lin et al., Loss-of-function analyses defines vital and redundant functions of the *Plasmodium* rhomboid protease family. *Mol. Microbiol.* **88**, 318–338 (2013).

32. B. Douradinha et al., *Plasmodium* cysteine repeat modular proteins 3 and 4 are essential for malaria parasite transmission from the mosquito to the host. *Malar. J.* **10**, 71 (2011).

33. A. A. Sultan et al., TRAP is necessary for gliding motility and infectivity of *Plasmodium* sporozoites. *Cell* **90**, 511–522 (1997).

34. L. N. Pham, M. S. Dionne, M. Shirasu-Hiza, D. S. Schneider, A specific primed immune response in *Drosophila* is dependent on phagocytes. *PLoS Pathog.* **3**, e26 (2007).

35. M. Povelones, R. M. Waterhouse, F. C. Kafatos, G. K. Christophides, Leucine-rich repeat protein complex activates mosquito complement in defense against *Plasmodium* parasites. *Science* **324**, 258–261 (2009).

36. A. S. Aly, K. Matuschewski, A malarial cysteine protease is necessary for *Plasmodium* sporozoite egress from oocysts. *J. Exp. Med.* **202**, 225–230 (2005).

37. A. Coppi et al., The malaria circumsporozoite protein has two functional domains, each with distinct roles as sporozoites journey from mosquito to mammalian host. *J. Exp. Med.* **208**, 341–356 (2011).

38. N. K. Kisalu et al., A human monoclonal antibody prevents malaria infection by targeting a new site of vulnerability on the parasite. *Nat. Med.* **24**, 408–416 (2018).

39. N. Yoshida, P. Potocnjak, V. Nussenzweig, R. S. Nussenzweig, Biosynthesis of Pb44, the protective antigen of sporozoites of *Plasmodium berghei. J. Exp. Med.* **154**, 1225–1236 (1981).

40. A. H. Cochrane, F. Santoro, V. Nussenzweig, R. W. Gwadz, R. S. Nussenzweig, Monoclonal antibodies identify the protective antigens of sporozoites of *Plasmodium knowlesi. Proc. Natl. Acad. Sci. U.S.A.* **79**, 5651–5655 (1982).

41. A. Coppi, C. Pinzon-Ortiz, C. Hutter, P. Sinnis, The *Plasmodium* circumsporozoite protein is proteolytically processed during cell invasion. *J. Exp. Med.* **201**, 27–33 (2005).

42. A. Molina-Cruz, G. E. Canepa, C. Barillas-Mury, *Plasmodium* P47: A key gene for malaria transmission by mosquito vectors. *Curr. Opin. Microbiol.* **40**, 168–174 (2017).

43. A. Molina-Cruz et al., The human malaria parasite Pfs47 gene mediates evasion of the mosquito immune system. *Science* **340**, 984–987 (2013).

44. U. N. Ramphul, L. S. Garver, A. Molina-Cruz, G. E. Canepa, C. Barillas-Mury, *Plasmodium falciparum* evades mosquito immunity by disrupting JNK-mediated apoptosis of invaded midgut cells. *Proc. Natl. Acad. Sci. U.S.A.* **112**, 1273–1280 (2015).

45. J. F. Hillyer, C. Barreau, K. D. Vernick, Efficiency of salivary gland invasion by malaria sporozoites is controlled by rapid sporozoite destruction in the mosquito haemocoel. *Int. J. Parasitol.* **37**, 673–681 (2007).

46. M. Loubens et al., *Plasmodium* sporozoites on the move: Switching from cell traversal to productive invasion of hepatocytes. *Mol. Microbiol.* **115**, 870–881 (2021).

47. P. E. Duffy, J. Patrick Gorres, Malaria vaccines since 2000: Progress, priorities, products. *NPJ Vaccines* **5**, 48 (2020).

48. L. Gonzalez-Ceron et al., *Plasmodium vivax*: A monoclonal antibody recognizes a circumsporozoite protein precursor on the sporozoite surface. *Exp. Parasitol.* **90**, 203–211 (1998).

49. S. E. Lindner et al., Transcriptomics and proteomics reveal two waves of translational repression during the maturation of malaria parasite sporozoites. *Nat. Commun.* **10**, 4964 (2019).

50. K. E. Swearingen et al., Proteogenomic analysis of the total and surface-exposed proteomes of *Plasmodium vivax* salivary gland sporozoites. *PLoS Negl. Trop. Dis.* **11**, e0005791 (2017).

51. K. E. Boysen, K. Matuschewski, Inhibitor of cysteine proteases is critical for motility and infectivity of *Plasmodium* sporozoites. *mBio* **4**, e00874-13 (2013).

52. M. J. Stewart, J. P. Vanderberg, Malaria sporozoites release circumsporozoite protein from their apical end and translocate it along their surface. *J. Protozool.* **38**, 411–421 (1991).

53. S. A. Arredondo, A. Schepis, L. Reynolds, S. H. I. Kappe, Secretory organelle function in the *Plasmodium* sporozoite. *Trends Parasitol.* **37**, 651–663 (2021).

54. R. Tewari, R. Spaccapelo, F. Bistoni, A. A. Holder, A. Crisanti, Function of region I and II adhesive motifs of *Plasmodium falciparum* circumsporozoite protein in sporozoite motility and infectivity. *J. Biol. Chem.* **277**, 47613–47618 (2002).

55. M. E. W. Logtenberg, F. A. Scheeren, T. N. Schumacher, The CD47-SIRPα immune checkpoint. *Immunity* **52**, 742–752 (2020).

56. M. Prado et al., Long-term live imaging reveals cytosolic immune responses of host hepatocytes against *Plasmodium* infection and parasite escape mechanisms. *Autophagy* **11**, 1561–1579 (2015).

57. T. Ponnudurai, A. D. Leeuwenberg, J. H. Meuwissen, Chloroquine sensitivity of isolates of *Plasmodium falciparum* adapted to in vitro culture. *Trop. Geogr. Med.* **33**, 50–54 (1981).

58. J. J. Campanella, L. Bitincka, J. Smalley, MatGAT: An application that generates similarity/identity matrices using protein or DNA sequences. *BMC Bioinformatics* **4**, 29 (2003).

59. J. Yang, Y. Zhang, I-TASSER server: New development for protein structure and function predictions. *Nucleic Acids Res.* **43**, W174–W181 (2015).

60. C. Zhang, P. L. Freddolino, Y. Zhang, COFACTOR: Improved protein function prediction by combining structure, sequence and protein-protein interaction information. *Nucleic Acids Res.* **45**, W291–W299 (2017).

61. C. J. Janse, J. Ramesar, A. P. Waters, High-efficiency transfection and drug selection of genetically transformed blood stages of the rodent malaria parasite *Plasmodium berghei. Nat. Protoc.* **1**, 346–356 (2006).

62. A. R. Gomes et al., A genome-scale vector resource enables high-throughput reverse genetic screening in a malaria parasite. *Cell Host Microbe* **17**, 404–413 (2015).

63. F. Schwach et al., PlasmoGEM, a database supporting a community resource for large-scale experimental genetics in malaria parasites. *Nucleic Acids Res.* **43**, D1176–D1182 (2015).

64. A. M. Salman et al., Generation of transgenic rodent malaria parasites expressing human malaria parasite proteins. *Methods Mol. Biol.* **1325**, 257–286 (2015).

65. C. Marin-Mogollon et al., Chimeric *Plasmodium falciparum* parasites expressing *Plasmodium vivax* circumsporozoite protein fail to produce salivary gland sporozoites. *Malar. J.* **17**, 288 (2018).

66. R. Spaccapelo et al., Plasmepsin 4-deficient *Plasmodium berghei* are virulence attenuated and induce protective immunity against experimental malaria. *Am. J. Pathol.* **176**, 205–217 (2010).

67. C. J. Janse et al., In vitro formation of ookinetes and functional maturity of *Plasmodium berghei* gametocytes. *Parasitology* **91**, 19–29 (1985).

68. C. M. Mogollon et al., Rapid generation of marker-free *P. falciparum* fluorescent reporter lines using modified CRISPR/Cas9 constructs and selection protocol. *PLoS One* **11**, e0168362 (2016).

69. T. Ponnudurai et al., Infectivity of cultured *Plasmodium falciparum* gametocytes to mosquitoes. *Parasitology* **98**, 165–173 (1989).

70. R. Sinden, "Infection of mosquitoes with rodent malaria" in *The Molecular Biology of Insect Disease Vectors*, C. B. Beard, J. M. Crampton, C. Louis, Eds. (Springer, Dordrecht, The Netherlands, 1997), pp. 67–91.